



Electronic structure and conformational isomerism of the digermene $(t\text{Bu}_2\text{MeSi})_2\text{Ge}=\text{Ge}(\text{SiMetBu}_2)_2$ as studied by temperature-dependent Raman and UV–vis spectra and quantum-chemistry calculations

Rinat R. Aysin^a, Sergey S. Bukalov^a, Larissa A. Leites^{a, **}, Vladimir Ya Lee^{b, *}, Akira Sekiguchi^{b, ***}

^a A. N. Nesmeyanov Institute of Organoelement Compounds, Scientific and Technical Center on Raman Spectroscopy, Russian Academy of Sciences, 28 Vavilova Str., 119991, Moscow, Russia

^b Department of Chemistry, Graduate School of Pure and Applied Sciences, University of Tsukuba, Tsukuba, 305-8571, Ibaraki, Japan

ARTICLE INFO

Article history:

Received 26 December 2018

Received in revised form

28 March 2019

Accepted 12 April 2019

Available online 22 April 2019

Keywords:

Digermene

Photodissociation

Raman

UV–vis spectroscopy

NCA

TD DFT

QTAIM calculations

ABSTRACT

The structure of the digermene $(t\text{Bu}_2\text{MeSi})_2\text{Ge}=\text{Ge}(\text{SiMetBu}_2)_2$ (**1**) was investigated by experimental (Raman and UV–vis) as well as computational (NCA, TD DFT and QTAIM) methods. Temperature-dependent Raman and UV–vis spectra have demonstrated that **1** does not dissociate into the corresponding germynes on heating either to 120 °C as a solid or to 80 °C in solution, thus preserving the integrity of its double Ge=Ge bond. Raman and NCA results allowed one to estimate the region of the $\nu_{\text{Ge}=\text{Ge}}$ vibrational frequency in the spectra of digermenes as 270–340 cm^{-1} . When illuminated with a red laser beam of enhanced power (>5 mW), solid **1** undergoes a transformation followed by disappearance of the $\nu_{\text{Ge}=\text{Ge}}$ Raman band. This process is evidently photodissociation caused by proximity of the red laser wavelength 632.8 nm to the intrinsic absorption of **1** at 616 nm. Temperature dependence of the Raman spectrum has revealed conformational isomerism in solid digermene **1** due to hindered rotation about the Ge–Si bonds, the conformers differing in mutual disposition of Me and bulky *t*Bu groups.

© 2019 Elsevier B.V. All rights reserved.

1. Introduction

Digermene $(t\text{Bu}_2\text{MeSi})_2\text{Ge}=\text{Ge}(\text{SiMetBu}_2)_2$ (**1**) was recently described [1] as sapphire-blue crystalline compound, thermally stable but air-sensitive; its synthesis, X-ray structure, electrochemical properties, and reactivity were reported therewith. It appeared to be a rather unusual example of a digermene featuring planar geometry at the doubly bonded germanium atoms and strongly twisted Ge=Ge bond, caused by the electronic and steric factors of the bulky σ -donating silyl substituents. Compound **1**, unlike many other digermenes (see the reviews [2] and the papers [3–5]), was shown not to dissociate into corresponding germynes in solution at room temperature. In this paper we provide full

account of the temperature-dependent Raman and UV–vis data for **1** and the results of quantum-chemistry calculations on **1** and model digermene systems (geometry optimization, QTAIM and NCA analysis, TDDFT) aimed to further elucidation of **1** electronic structure and reactivity.

2. Experimental

All experimental manipulations involving **1** were performed either using standard Schlenk-line techniques or under an argon atmosphere of a MBRAUN glove box.

UV–vis spectra in the region 200–900 nm were recorded on a UV–vis spectrophotometer Carl Zeiss Specord M400 for solid **1** at room temperature (as an Apiezon mull and thin film formed from a solution in hexane) as well as its solution in liquid Nujol (paraffin oil) in the temperature interval from 20 to 80 °C.

Raman spectra in the region 100–4000 cm^{-1} were registered using a laser Raman spectrometer Horiba JobinYvon LabRAM 300 with 632.8 nm excitation of a He-Ne laser with particular attention

* Corresponding author.

** Corresponding author.

*** Corresponding author.

E-mail addresses: buklei@ineos.ac.ru (L.A. Leites), leevya@chem.tsukuba.ac.jp (V.Y. Lee), a.sekiguchi@aist.go.jp (A. Sekiguchi).

to the laser power (see below). For the Raman measurements, a special cell was fabricated representing a round metal plate with a deepening 0.3 mm thick, in which the sample was placed under an inert atmosphere with a glass cover glued above. This cell was settled in a temperature setup Linkam THMS-600.

3. Calculations

Geometry optimization, normal coordinate analysis (NCA) in harmonic approximation, calculations of thermodynamic parameters and of low-energy electronic transitions were carried out at DFT level with PBE0 [6] and TPSS [7] functionals using ORCA (version 4) program [8]. In recent years, it is considered necessary to introduce dispersion correction D3BJ [9]. As molecule **1** contains bulky *t*Bu groups in close contact, dispersion correction to energy seems to be significant. However, we have found that introduction of this correction leads to overestimation of dissociation energy which contradicts to the experimental results. For additional refinement of calculation, relativistic effect corrections were entered in the zeroth order regular approximation (ZORA) [10] with ZORA-def2-TZVP basis set [11]. As the objects of calculation are huge, to accelerate the process we utilized the RIJCOSX [12] approximation with def2/J fitting basis set [13]. The choice of a level of computation depended on proximity of the computed values to the experimental ones (geometry parameters, vibrational frequencies and position of π - π^* transition, see below). PBE0 (without D3BJ) was used for estimation of relative energies whereas TPSS for normal coordinate analysis (NCA). QTAIM analysis [14] of electron density was done at the PBE0/Def2-TZVP level using AIMAll program [15]. Time-dependent (TD) DFT calculations were performed at the same level on 20 highest electronic excitations.

4. Results and discussion

4.1. Geometry optimization of **1** and model digermenes

In the previous papers [1], the following data on the geometry of **1** based on the X-ray diffraction results were reported: a Ge=Ge bond distance ($r_{\text{Ge}=\text{Ge}}$) of 2.346 (2) Å and nearly planar geometry around the Ge centers with the sum of the bond angles totaling 358.8° and 359.2°. Similar values are characteristic for other tetrasilyldigermenes [16]. However, unlike the latter, the Ge=Ge bond in **1** is extraordinarily twisted (twisting angle δ was reported as 52.8°), which was reasonably ascribed to the great steric constraint caused by the voluminous *t*Bu₂MeSi substituents. We have carried out geometry optimization for **1** using two levels of theory, the results obtained are presented in Table 1. It is important to note that all calculations show that in molecule **1** there are two different torsional angles around the Ge=Ge bond, their particular values appeared sensitive towards the computational level due to shallow potential energy surface for **1** (the shorter the Ge=Ge bond, the bigger the difference between the two torsional angles). A similar result (two different torsional angles 48.8 and 62.9°) was obtained by X-ray diffraction for a disilene molecule **2** with the same substituents *t*Bu₂MeSi as in **1** [17], this disilene also having a close value of the twisting angle $\delta = 54.5^\circ$. The asymmetry of molecule **1** is reflected by an asymmetry in the Ge–Si bonding (see Table 1); for comparison: the lengths of the Ge–Si bonds in **1** range from 2.432 (4) Å to 2.464 (4) Å, as was determined by its X-ray crystallography.

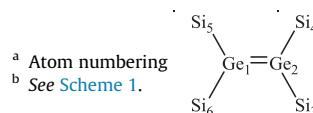
4.2. UV–vis results

Digermene **1** in hexane solution was reported [1] to exhibit in its electronic spectrum the longest wavelength absorption at 618 nm as compared to substantially smaller values 413–472 nm of other

Table 1

The results of geometry optimization for **1** (exp. $r_{\text{Ge}=\text{Ge}} = 2.346$ (2) Å, $\delta = 52.8^\circ$).

Molecule ^a	1 (conformer a) ^b		1 (conformer c) ^b	
	PBE0	TPSS D3BJ	PBE0	TPSS D3BJ
Salient geometry parameters				
$r_{\text{Ge}_1=\text{Ge}_2}$, Å	2.346	2.330	2.330	2.324
$r_{\text{Ge}_2-\text{Si}_3}$, Å	2.486	2.451	2.471	2.440
$r_{\text{Ge}_2-\text{Si}_4}$, Å	2.480	2.441	2.453	2.435
$r_{\text{Ge}_1-\text{Si}_5}$, Å	2.465	2.415	2.488	2.439
$r_{\text{Ge}_1-\text{Si}_6}$, Å	2.453	2.424	2.485	2.435
$\text{Si}_3-\text{Ge}_2=\text{Ge}_1-\text{Si}_6$, deg	57.8	52.8	43.8	39.5
$\text{Si}_4-\text{Ge}_2=\text{Ge}_1-\text{Si}_5$, deg	64.2	68.7	56.4	70.3
twist angle δ , deg	61.1	60.9	49.2	52.4
Si-Ge-Si, deg	130.1	130.7	115.4	118.7
	129.0	130.0	117.5	



much less sterically congested tetrasilyldigermenes [16]. The only equally high value, that at 612 nm, was observed for the disilene **2** [17], the molecule **2** being similar to **1** also in other respects.

We have obtained the same band at ~616 nm for the room-temperature spectra of solid **1** (Fig. 1) and for its solution in paraffin oil.

In the course of temperature study of the solution, on gradual heating it to 80 °C, this band did not alter significantly, exhibiting a natural slight red shift and broadening. Our TD-DFT results confirm the assignment of this band to the π - π^* transition. The calculated value for this transition is 619 nm, in a very good accord with the experiment. Calculation for the n–p transition on the corresponding germylene (*t*Bu₂MeSi)₂Ge: resulted in a much longer wavelength 680 nm. We did not observe a feature in the latter region in the experimental UV–vis spectra even on heating up to 80 °C. This finding along with the Raman data (see below) allowed us to confirm the inference [1] that **1** does not dissociate into the germylenes and retains the integrity of its Ge=Ge bond, this conclusion being extended now to higher temperatures. It is pertinent to

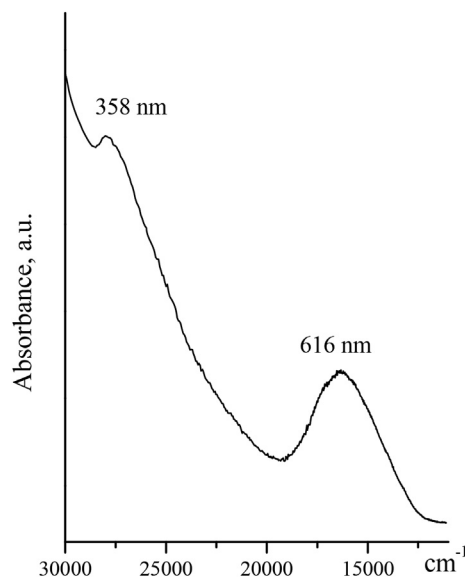


Fig. 1. UV–vis spectrum of solid **1** at room temperature.

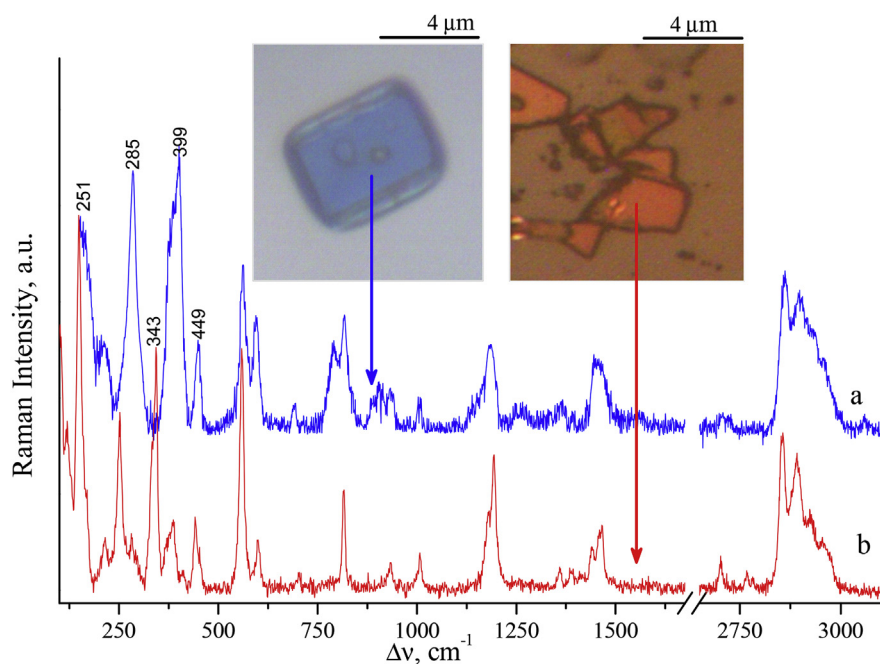


Fig. 2. (a) Initial Raman spectrum of a blue microcrystal of **1** (see left photo) at room temperature; (b) the spectrum of a sample which changed its color upon intense illumination (see right photo and the text). (For interpretation of the references to colour in this figure legend, the reader is referred to the Web version of this article.)

note that positive values of enthalpy ΔH and the Gibbs free energy ΔG for dissociation of **1** into two germylenes, calculated as 25.1 and 8.3 kcal/mol at PBE0 level, respectively, confirm that this reaction is unfavourable.

4.3. On vibrations of the Ge=Ge bond in the spectra of digermenes

The data on the stretching vibration of the Ge=Ge bond are very limited. In the papers of Lappert et al. [5] an intense polarized Raman line at 300 cm^{-1} was attributed to $\nu_{\text{Ge=Ge}}$ in the corresponding digermene $[(\text{Me}_3\text{Si})_2\text{CH}]_2\text{Ge=Ge}[\text{CH}(\text{SiMe}_3)_2]$. An intense line at 340 cm^{-1} in the spectrum of solid 1,2-bis(ferrocenyl)digermene FcTipGe=GeTipFc (Fc = ferrocene, Tip = 2,4,6-triisopropylphenyl) was reported as $\nu_{\text{Ge=Ge}}$ vibration by Tokitoh et al. [18]. Both assignments seem reasonable. However, as the authors [5b] pointed to decomposition of their digermene in the Kr^+ laser beam and given the well-known intense sharp Raman line of crystalline Ge with frequency just at 300 cm^{-1} [19], one cannot completely rule out that the line at 300 cm^{-1} observed in Ref. [5] could be due to germanium formed during the decomposition of that compound in the intense laser beam. Decomposition of germanium-containing organometallics with formation and deposition of metallic Ge is well-known (see e.g. Ref. [20]). As for the data of Ref. [18], one could add that the vibrational spectra of ferrocene and its derivatives exhibit intense features just in the region $300\text{--}400\text{ cm}^{-1}$ [21], which makes unambiguous assignment of the observed vibration at 340 cm^{-1} difficult. The vibrational spectrum of matrix-isolated digermene $\text{Me}_2\text{Ge=GeMe}_2$ at 5 K was published in Ref. [22] and the $\nu_{\text{Ge=Ge}}$ vibration was assigned as the line at 404 cm^{-1} , that is, $\sim 100\text{ cm}^{-1}$ higher than those reported [5,18]. Thus it was of interest to elucidate and substantiate the region of $\nu_{\text{Ge=Ge}}$ mode, the dependence of its frequency on the nature of substituents and molecular geometry as well as to determine eigenvectors of these normal modes. For this, the complete Raman spectrum of solid digermene $(t\text{Bu}_2\text{MeSi})_2\text{Ge=Ge}(\text{SiMe}_2\text{tBu})_2$ (**1**) was registered (for the room-temperature spectrum see Fig. 2a) and calculations of normal mode

frequencies and eigenvectors (NCA) were performed. Comparison of experimental and computed data for **1** with the band assignment are given in Table 2.

Molecule **1** contains 126 atoms, thus, formally speaking, its vibrational spectrum must exhibit 372 fundamentals. The molecule possess no symmetry elements, hence all its vibrations should be Raman-active. However, vast experience in vibrational spectroscopy of organometallics has shown that internal vibrations of the identical substituents do not interact kinematically through the heavier metal atoms, leading to a great simplification of the spectrum. Indeed, examination of the experimental Raman spectrum of **1** along with the NCA results show that the frequencies of the normal modes with similar eigenvectors nearly coincide. The

Table 2

Experimental and computed Raman spectrum of **1** and normal mode assignment based on NCA results.

Raman exp. for 1	Calc (TPSS-D3BJ)	normal mode assignment
215 m		τCH_3
285vs	273–299	$\nu_{\text{Ge=Ge}} - \nu_{\text{Ge-Si}} + \tau\text{CH}_3$
387sh/399vs	350–380	$\nu^{\text{as}}\text{Ge-Si} + \delta\text{TMS}$
450 m	390–420	$\nu^{\text{as}}\text{Ge-Si} + \delta\text{TMS}$
486/mw		
561s	520–528	$\nu^{\text{s}}\text{Si-C}$
594 ms	562–567	$\nu^{\text{as}}\text{Si-C}$
690w	672–687	$\nu\text{Si-CH}_3$
789 m	769–793	ρCH_3
813s		$\nu^{\text{s}}\text{C-C}(\text{tBu})$
890sh	797–804	
907, 935w	916–931	$\nu^{\text{as}}\text{C-C}(\text{tBu}) + \rho\text{CH}_3$
1005w		
1157sh		
1186 ms		
1250w		$\delta^{\text{s}}\text{CH}_3$
1270vw		
1368w		
1445/1462		$\delta^{\text{as}}\text{CH}_3$
2857		
2895		$\nu\text{C-H}$
2936		

Table 3
Experimental and calculated $\nu_{\text{Ge}=\text{Ge}}$ frequencies and geometry parameters.

Molecule	$\nu_{\text{Ge}=\text{Ge}}$, cm^{-1}		Dihedral angles	$r_{\text{Ge}=\text{Ge}}$	Comment
	calc.	exp.	calc.		
$\text{Me}_2\text{Ge}=\text{GeMe}_2$	268	404 [22]	54	2.315	PED ^a 80% $\nu_{\text{Ge}=\text{Ge}}$
$[\text{Me}_3\text{Si}]_2\text{CH}_2\text{Ge}=\text{Ge}[\text{CH}(\text{SiMe}_3)_2]_2$	289	300 [5]	47, 27	2.348	
$(t\text{Bu}_2\text{CH})_2\text{Ge}=\text{Ge}(\text{CH}t\text{Bu}_2)_2$	318–324		30, 12	2.318	
$(t\text{Bu}_2\text{HSi})_2\text{Ge}=\text{Ge}(\text{Si}t\text{Bu}_2)_2$	319–322		35, 4	2.270	
$(t\text{Bu}_2\text{MeSi})_2\text{Ge}=\text{Ge}(\text{Si}t\text{Me}t\text{Bu}_2)_2$	273–299	285	69, 53	2.330	

^a PED – potential energy distribution.

spectrum is clearly subdivided into the frequency regions corresponding to normal modes with close frequencies and eigenvectors. This allows us to make an assignment given in Table 2.

Thus we can unambiguously assign the intense line at 285 cm^{-1} in the experimental spectrum of **1** to the assembly of normal modes with predominant contribution from the $\text{Ge}=\text{Ge}$ stretching coordinate, or simply to $\nu_{\text{Ge}=\text{Ge}}$. The calculated frequency region for these modes is $273\text{--}299\text{ cm}^{-1}$, in close fit with the experimental frequency. The same is true of the totally symmetric $\nu_{\text{Ge}=\text{Si}}$ stretches (exp. value 399 , calc. $350\text{--}380\text{ cm}^{-1}$). These facts speak for adequacy of the computation level used. It is necessary to note that the $\nu_{\text{Ge}=\text{Ge}}$ mode is not well-localized being mixed to some extent with the $\nu_{\text{Ge}=\text{Si}}$ stretches and angle deformations.

To check the literature data, NCA calculations were also carried out for the C-substituted digermenes, namely $\text{Me}_2\text{Ge}=\text{GeMe}_2$ [22] and Lappert's digermene $[(\text{Me}_3\text{Si})_2\text{CH}]_2\text{Ge}=\text{Ge}[\text{CH}(\text{SiMe}_3)_2]_2$ [5]. Comparison of the salient geometry parameters and the $\nu_{\text{Ge}=\text{Ge}}$ frequencies of various digermenes calculated at ZORA-TPSS-D3BJ level is presented in Table 3.

The NCA results for the simplest C-substituted digermene $\text{Me}_2\text{Ge}=\text{GeMe}_2$ (**3**) appeared unexpected and allowed us to make a question of the data [22]. Geometry optimization for **3** resulted in a bent skeleton of C_{2h} symmetry with $r_{\text{Ge}=\text{Ge}}$ 2.315 \AA , $\delta \sim 54^\circ$. The calculated $\nu_{\text{Ge}=\text{Ge}}$ frequency is 268 cm^{-1} , thus having nothing in common with the value 404 cm^{-1} reported [22]. The same is true of the $\nu_{\text{Ge}=\text{C}}$ modes, their computed frequencies lying in the region $530\text{--}560\text{ cm}^{-1}$, while those reported for **3** at $580\text{--}590\text{ cm}^{-1}$. Such a huge difference cannot be attributed to computational error. From these facts it follows that the spectrum reported [22] did not belong to digermene **3**. It is noteworthy that the line near 400 cm^{-1} is present in the spectrum of naphthalene, which is formed along with **3** as a result of thermal decomposition of the starting digermabicyclooctadiene [22]. The calculations for the Lappert's digermene resulted in $r_{\text{Ge}=\text{Ge}}$ 2.348 \AA and the frequency of $\nu_{\text{Ge}=\text{Ge}}$ at 289 cm^{-1} , in good accord with the experimental values [5]. Thus the NCA results obtained have evidenced that the $\nu_{\text{Ge}=\text{Ge}}$ mode frequency is situated in the region $260\text{--}340\text{ cm}^{-1}$ for both C- and Si-substituted digermenes. Its value is not correlated directly with the bond length but is determined by molecular geometry and by particular mode eigenvector. Remarkably, this frequency region is not far from that corresponding to $\nu_{\text{Ge}=\text{Ge}}$ single bond in the spectra of digermane [23], polygermanes [24] and amorphous Ge [19]. However, all these frequency values cannot be taken as a measure of bond connectivity, because all these vibrations are not localized in the germanium-germanium bond, being strongly mixed with those of neighbouring bonds and angles.

4.4. Transformation of compound **1** in the red laser beam in the course of Raman spectrum registration

When we obtained the Raman spectrum of **1** using red excitation with laser power values less than 0.5 mW , the microcrystalline sample of **1** monitored on a screen under the microscope preserved

its blue colour, giving a constant Raman spectrum presented in Fig. 2a. However, at higher laser power values, the sample region illuminated by the laser beam has irreversibly changed its colour to yellow-red, exhibiting another spectrum (see Fig. 2b) and thus indicating irreversible transformation of digermene **1** into other compounds. In the latter spectrum, the band corresponding to the $\text{Ge}=\text{Ge}$ bond disappeared while the bands corresponding to alkyl groups grew in relative intensity. By analogy with the literature data, we can suppose that under these conditions **1** undergoes dissociation of the $\text{Ge}=\text{Ge}$ bond with subsequent reactions of the germylene formed. The reason of this process is evidently photochemistry, because the exciting line used (632.8 nm) is near to the substance inherent absorption (618 nm). This process is obviously not thermo-destruction because heating of the sample to 120°C with use of low laser power (less than 0.5 mW) does not destroy the blue sample (see below). Currently it is impossible to specify the complex mixture of the products of subsequent reactions by means of only Raman spectroscopy, but appearance of the lines at 251 and 343 cm^{-1} in the spectrum of the red-yellow product (Fig. 2b) suggests formation of corresponding Si-substituted oligogermanes (computed frequency values for an infinite polymer with $-\text{Si}_2\text{Ge}=\text{GeSi}_2-$ backbone are 240 and 330 cm^{-1}).

4.5. Temperature dependence of the Raman spectrum

Temperature dependence of the Raman spectrum in the region of $\nu_{\text{Ge}=\text{Ge}}$ and $\nu_{\text{Ge}=\text{Si}}$ vibrations ($250\text{--}450\text{ cm}^{-1}$) in the interval $20\text{--}120^\circ\text{C}$ is presented in detail in Fig. 3. It can be seen that the band corresponding to the $\nu_{\text{Ge}=\text{Ge}}$ vibration at $\sim 285\text{ cm}^{-1}$ does not change with temperature while the band in the region $370\text{--}400\text{ cm}^{-1}$, corresponding to the $\nu_{\text{Ge}=\text{Si}}$ symmetric stretch,

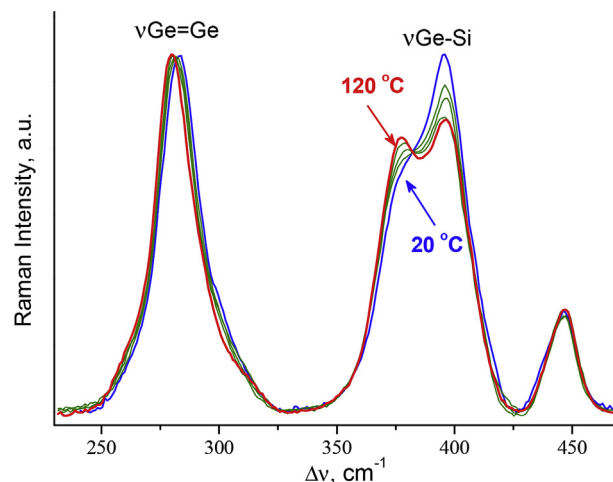
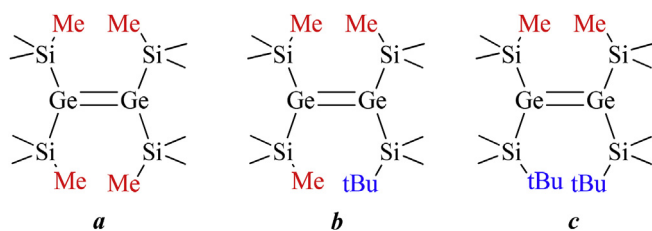


Fig. 3. Reversible temperature dependence of the Raman spectrum of solid **1** in the region of $\nu_{\text{Ge}=\text{Ge}}$ and $\nu_{\text{Ge}=\text{Si}}$ vibrations.



Scheme 1. Possible conformers of molecule **1**.

appeared a doublet with components at 377 and 399 cm^{-1} whose intensity ratio depends on temperature, the former band intensity raising on heating while that of the latter decreasing. The process is reversible. A clear-cut isosbestic point observed in the spectral region of the $\nu_{\text{Ge-Si}}$ bands points to an equilibrium between two different sets of conformers apparently due to hindered rotation about the Ge-Si bonds.

This is quite understandable taking into account asymmetrical substitution at Si atoms and steric constraint caused by the presence of the two bulky *t*Bu groups at each Si atom. Conformational isomerism in the solid state is not without precedents, see *e.g.* Ref. [25]. Our geometry calculation at the DFT ZORA-PBE0 level has optimized the conformer **a** (“in-in”) shown in Scheme 1 with the two methyl groups facing each other (the shortest calculated distance between the non-bonded H atoms of neighbouring Me groups is 2.0 Å). A small ΔG energy difference between the possible conformers computed within 2 kcal/mol limit agrees well with the equilibrium observed. The most stable conformers are shown in Scheme 1 (for details see Supplementary), and according to the results of our calculations, they differ in geometry and exhibit close values of the $\nu_{\text{Ge=Ge}}$ frequency but different values of the $\nu_{\text{Ge-Si}}$ frequency, in accord with the experimental Raman data.

4.6. QTAIM results

Topological parameters of electron density distribution obtained as a result of Bader's QTAIM analysis for some digermenes and a digermene are presented in Table 4. Examination of the data on the Ge=Ge bond shows that this bond is a typically covalent one, as expected, it is characterized by a negative value of the Laplacian at the (3,-1) bond critical point. Moreover, this parameter for the Ge-Si bonds suggests covalent interactions also for these bonds, which can be attributed to not very differing electronegativities of

Table 4
QTAIM parameters at ZORA-PBE0-RIJCOSX/Def2-TZVP level.

BCP	ρ_b , a.u.	$\nabla^2\rho$, a.u.	V, a.u.	G, a.u.	H, a.u.	$\delta(A,B)$
1a						
Ge ₁ =Ge ₂	0.085586	-0.053055	-0.070569	0.028653	-0.042	1.48
Ge ₂ -Si ₃	0.074028	-0.091342	-0.042808	0.009986	-0.033	0.69
Ge ₂ -Si ₄	0.074550	-0.093404	-0.043485	0.010067	-0.033	0.69
Ge ₁ -Si ₅	0.077764	-0.105179	-0.047384	0.010545	-0.037	0.69
Ge ₁ -Si ₆	0.076357	-0.099842	-0.045606	0.010323	-0.035	0.69
(Me ₃ Si) ₂ Ge=Ge(SiMe ₃) ₂						
Ge=Ge	0.096890	-0.061362	-0.089652	0.037156	+0.052	1.69
Ge-Si	0.086408	-0.148644	-0.062529	0.012684	+0.050	0.68
(H ₃ Si) ₂ Ge=Ge(SiH ₃) ₂						
Ge=Ge	0.099300	-0.064943	-0.093135	0.038449	-0.055	1.70
Ge-Si	0.088067	-0.147116	-0.075206	0.019213	-0.056	0.70
Me ₂ Ge=GeMe ₂						
Ge=Ge	0.092767	-0.061225	-0.081706	0.033200	-0.049	1.29
Ge-C	0.124100	+0.078568	-0.140651	0.080147	-0.061	0.85
Me ₃ Ge-GeMe ₃						
Ge-Ge	0.089416	-0.099787	-0.062147	0.018600	-0.043	0.76
Ge-C	0.125819	+0.094287	-0.146613	0.085092	-0.061	0.79

these two atoms. Small positive Laplacian values for Ge-C bonds in the digermene Me₂Ge=GeMe₂ and the digermene Me₃Ge-GeMe₃ correspond to their intermediate type. One of reliable bond parameters is delocalization index $\delta(A,B)$ [14] which formally corresponds to bond order. For single ordinary bonds this index usually does not reach unity. Indeed, in all the digermenes and a digermene studied the $\delta(A,B)$ values for Ge-Si and Ge-C bonds (Table 4) are less than unity. At the same time, the Ge=Ge bonds in all the digermenes exhibit $\delta(A,B)$ values greater than unity (1.29–1.7) and substantially greater than that for the single Ge-Ge bond in hexamethyldigermene (0.76). This clearly points to double-bond character of the Ge=Ge bond. Comparison of the QTAIM data (namely, $\delta(A,B)$ and ρ_b values) for three Si-substituted digermenes presented in Table 4 demonstrates weakening of the Ge=Ge bond on going from (H₃Si)₂Ge=Ge(SiH₃)₂ and (Me₃Si)₂Ge=Ge(SiMe₃)₂ to **1**, that is, with Ge=Ge bond elongation due to an increase in steric hindrance.

5. Conclusions

Based on the results of temperature investigation of the Raman and UV-vis spectra, digermene **1** does not dissociate into corresponding germylenes either on heating to 120 °C as a solid or on heating to 80 °C in solution. This conclusion is corroborated by the results of calculation of thermodynamic parameters of this reaction. However, when illuminated by a red laser beam of enhanced power (>5 mW), the blue digermene **1** transforms into a red-yellow substance. The process is accompanied by disappearance of the $\nu_{\text{Ge=Ge}}$ band in the Raman spectrum. This transformation is evidently due to a photodissociation of the digermene caused by proximity of the red laser wavelength 632.8 nm to the intrinsic absorption of the substance at 618 nm.

Temperature dependence of the Raman spectrum has shown that solid digermene **1** exists as an equilibrium mixture of several conformers due to hindered rotation about the Ge-Si bonds. The conformers differ in mutual disposition of Me and bulky *t*Bu groups in this sterically hindered molecule.

Conflicts of interest

There are no conflicts to declare.

Acknowledgement

The authors (RRA, SSB and LAL) acknowledge partial financial support from the Presidium of the Russian Academy of Sciences (program # 0085-2018-0008). The authors (VYL and AS) acknowledge financial support by the JSPS KAKENHI Grants program (nos. JP18K05137 and JP16K05682) from the Ministry of Education, Science, Sports, and Culture of Japan.

Appendix A. Supplementary data

Supplementary data to this article can be found online at <https://doi.org/10.1016/j.jorganchem.2019.04.014>.

References

- [1] (a) V.Ya Lee, K. McNeice, Y. Ito, A. Sekiguchi, Chem. Commun. 47 (2011) 3272–3274. <https://doi.org/10.1039/c0cc05415a>;
(b) V.Ya Lee, K. McNeice, Y. Ito, A. Sekiguchi, N. Geinik, J.Y. Becker, Heteroat. Chem. 25 (2014) 313–319. <https://doi.org/10.1002/hc.21165>.
- [2] For recent reviews, see: (a) Y. Mizuhata, T. Sasamori, N. Tokitoh, Chem. Rev. 109 (2009) 3479. <https://doi.org/10.1021/cr900093s>;
(b) V.Ya Lee, A. Sekiguchi, in: Organometallic Compounds of Low-Coordinate Si, Ge, Sn, Pb: from Phantom Species to Stable Compounds, Wiley, Chichester, UK, 2010. Ch. 5. <https://doi.org/10.1002/9780470669266.ch5>;

- (c) V.Ya Lee, A. Sekiguchi, in: J. Reedijk, K. Poeppelemeier (Eds.), *Comprehensive Inorganic Chemistry II*, Elsevier: Oxford, UK vol. 1, 2013, p. 289, Ch. 1.11.
- [3] N. Hayakawa, T. Sugahara, Y. Numata, H. Kawaai, K. Yamatani, Sh Nishimura, Sh Goda, Y. Suzuki, T. Tanikawa, H. Nakai, D. Hashizume, T. Sasamori, N. Tokitoh, T. Matsuo, *Dalton Trans.* 47 (2018) 814–822. <https://doi.org/10.1039/C7DT03819Ds>.
- [4] N. Tokitoh, K. Kishikawa, R. Okazaki, T. Sasamori, N. Nakata, N. Takeda, *Polyhedron* 21 (2002) 563–577. [https://doi.org/10.1016/S0277-5387\(01\)01035-X](https://doi.org/10.1016/S0277-5387(01)01035-X).
- [5] (a) D.E. Goldberg, D.H. Harris, M.F. Lappert, K.M. Thomas, *J. Chem. Soc., Chem. Commun.* (1976) 261. <https://doi.org/10.1039/C39760000261>;
(b) P.J. Davidson, D.H. Harris, M.F. Lappert, *J. Chem. Soc. Dalton Trans.* (1976) 2268. <https://doi.org/10.1039/DT97600002268>;
(c) T. Fjeldberg, A. Haaland, B.E.R. Schilling, M.F. Lappert, A.J. Thorne, *J. Chem. Soc., Dalton Trans.* (1986) 1551–1556. <https://doi.org/10.1039/DT98600001551>;
(d) D.E. Goldberg, P.B. Hitchcock, M.F. Lappert, K.M. Thomas, A.J. Thorne, T. Fjeldberg, A. Haaland, B.E.R. Schilling, *J. Chem. Soc., Dalton Trans.* 1986, pp. 2387–2394. <https://doi.org/10.1039/DT98600002387>.
- [6] C. Adamo, V. Barone, *J. Chem. Phys.* 110 (1999) 6158–6169. <https://doi.org/10.1063/1.478522>.
- [7] J. Tao, J.P. Perdew, V.N. Staroverov, G.E. Scuseria, *Phys. Rev. Lett.* 91 (2003) 146401. <https://doi.org/10.1103/PhysRevLett.91.146401>.
- [8] F. Neese, The ORCA program system, *WIREs Comput. Mol. Sci.* 2 (2012) 73–78. <https://doi.org/10.1002/wcms.81>.
- [9] (a) S. Grimme, S. Ehrlich, L. Goerigk, *J. Comput. Chem.* 32 (2011) 1456–1465. <https://doi.org/10.1002/jcc.21759>;
(b) S. Grimme, J. Antony, S. Ehrlich, H. Krieg, *J. Chem. Phys.* 132 (2010) 154104. <https://doi.org/10.1063/1.3382344>.
- [10] C. van Wuelen, *J. Chem. Phys.* 109 (1998) 392–399. <https://doi.org/10.1063/1.476576>.
- [11] F. Weigend, R. Ahlrichs, *Phys. Chem. Chem. Phys.* 7 (2005) 3297–3305. <https://doi.org/10.1039/B508541A>.
- [12] F. Neese, *J. Comput. Chem.* 24 (2003) 1740–1747. <https://doi.org/10.1002/jcc.10318>;
- (b) F. Neese, F. Wennmohs, A. Hansen, U. Becker, *Chem. Phys.* 356 (2009) 98–109. <https://doi.org/10.1016/j.chemphys.2008.10.036>;
- (c) A.K. Dutta, F. Neese, R. Izsak, *J. Chem. Phys.* 144 (2016), 034102. <https://doi.org/10.1063/1.4939844>.
- [13] F. Weigend, *Phys. Chem. Chem. Phys.* 8 (2006) 1057–1065. <https://doi.org/10.1039/B515623H>.
- [14] R.F.W. Bader, *Atoms in Molecules: A Quantum Theory*, Oxford Univ. Press, Oxford, 1990.
- [15] AIMAll (Version 17.11.14), A. Todd, T.K. Keith, Gristmill Software, Overland Park KS, USA, 2017 (aim.tkgristmill.com).
- [16] M. Kira, T. Iwamoto, T. Maruyama, C. Kabuto, H. Sakurai, *Organometallics* 15 (1996) 3767–3769. <https://doi.org/10.1021/om960370p>.
- [17] A. Sekiguchi, S. Inoue, M. Ichinohe, Y. Arai, *J. Am. Chem. Soc.* 126 (2004) 9626–9629. <https://doi.org/10.1021/ja040079y>.
- [18] T. Sasamori, H. Miyamoto, H. Sakai, Y. Furukawa, N. Tokitoh, *Organometallics* 31 (2012) 3904–3910. <https://doi.org/10.1021/om990337d>.
- [19] (a) J.H. Parker Jr., D.W. Feldman, M. Ashkin, *Phys. Rev.* 155 (1967) 712–714. <https://doi.org/10.1103/PhysRev.155.712>;
(b) M. Wakaki, M. Iwase, Y. Show, K. Koyama, S. Sato, S. Nozaki, H. Morisaki, *Physica B* 219/220 (1996) 535–537. [https://doi.org/10.1016/0921-4526\(95\)00803-9](https://doi.org/10.1016/0921-4526(95)00803-9).
- [20] S. S. Bukalov, L.A. Mikhailitsyn, L.A. Leites, G.A. Domrachev, E.G. Domracheva, B.S. Kaverin, A.M. Ob'edkov, *Mendeleev Commun.* (2003) 251–252. <https://doi.org/X0013251>.
- [21] E. Maslowsky, *Vibrational Spectra of Organometallic Compounds*, Wiley, NY, 1977, p. 315.
- [22] P. Bleckmann, R. Minkwitz, W.P. Neumann, M. Schriewer, M. Thibud, B. Watta, *Tetrahedron Lett.* 25 (1984) 2467–2470. [https://doi.org/10.1016/S0040-4039\(01\)81206-5](https://doi.org/10.1016/S0040-4039(01)81206-5).
- [23] B. Fontal, T.G. Spiro, *Inorg. Chem.* 10 (1971) 9–13. <https://doi.org/10.1021/ic50095a003>.
- [24] S.S. Bukalov, L.A. Leites, I.V. Krylova, M.P. Egorov, *J. Organomet. Chem.* 636 (2001) 164–171. [https://doi.org/10.1016/S0022-328X\(01\)01096-8](https://doi.org/10.1016/S0022-328X(01)01096-8).
- [25] S.S. Bukalov, R.R. Aysin, L.A. Leites, M.A. Kurykin, V.N. Khrustalev, *J. Mol. Struct.* 1098 (2015) 246–254. <https://doi.org/10.1016/j.molstruc.2015.06.002>.